



An Investigation the Effects of Geometric Tolerances on the Natural Frequencies of Rotating Shafts

Ali Akbar Ansarifard¹, Abdolrahman Jaamialahmadi²

¹MSc. Mechanical Student, Amirkabir University of Technology,
Hafez Street, Tehran, ansarifard165@aut.ac.ir,

²Assistant Prof. of Mechanical Engineering Department, Ferdowsi University of Mashhad,
Azadi Square, Mashhad, jaami-a@um.ac.ir

Received May 20 2014; revised August 24 2014; accepted for publication September 05 2014.
Corresponding author: Ali Akbar Ansarifard, ansarifard165@aut.ac.ir, ali.ansarifard@yahoo.com

Abstract

This paper examines the effects of geometric tolerances on the natural frequencies of rotating shafts. In order to model the tolerances, a code is written in MATLAB 2013 that produces deviated points. Deviated points are controlled by different geometric tolerances, including cylindricity, total run-out and coaxiality tolerances. Final surfaces and models passing through the points are created using SolidWorks 2013 and finally modal analysis is carried out with FE software. It is observed whenever the natural frequency is higher or the geometric tolerances are greater, natural frequencies of the real and ideal shafts are more distant. Also, the difference percentage between ideal and real frequencies is investigated. The results show that the percentage value is approximately constant for every mode shapes.

Keywords: Geometric tolerance, Natural frequency, Critical rotational speed, Rotating shafts, Modal analysis.

1. Introduction

Today, high rotational speed shafts are very applicable especially in rapid pump and turbomachinery industries. Investigating the natural frequency of rotating shafts is necessary in designing shafts. In order to comply with safety lines to prevent failure due to the deflections over the allowable limit, applying rotational speeds close to the critical speeds are avoided. In the manufacturing processes, creation of pieces with no tolerance in the view of dimension and geometry will be very difficult and expensive, and its value depends on the performance characteristics of the piece. In general, manufacturing the parts with relative motions compared to each other should be more accurate than the fixed parts. Moving parts are always being excited by the applied loads and if the frequency of the applied loads becomes equal to one of the natural frequencies of the moving parts, the resonance phenomenon occurs. Therefore, the manufacturing process should be performed in such a way that the final product be ever closer to the ideal target. Then natural frequencies of produced models can be estimated by obtaining natural frequencies of ideal models from the possible methods, and then necessary forecasts and preventions can be performed. These frequencies are known as the critical rotational speeds in rotating shafts. Today, the critical rotational speed is highly regarded and the damping system should be designed in such a way that it can damp the extremely large lateral forces acting on the bearings during the resonance.

When the rotational speed of rotating shafts is high, any defects and deviations in the geometry and material of the system could bring destructive events. A large number of researchers have studied the vibrations of rotating shafts considering the effects of different parameters such as misalignment, unbalancing, clearance and cracks. Xu and Maragani [1], for example, developed a theoretical model of a complete motor-flexible coupling-rotor system capable of describing the mechanical vibration resulting from misalignment and unbalance. They stated that the vibrations induced by misalignment are amplified into major vibration sources. They also validated the results by some experimental studies [2]. Lee et. al. [3] derived a dynamic model for misaligned rotor-ball bearing systems driven

through a flexible coupling by treating the reaction loads and deformations at the bearing and coupling elements as the misalignment effect. They showed as the angular misalignment increases, the whirling orbits tend to collapse toward a straight line, and the natural frequency of the misaligned rotor system associated with the misalignment direction increases largely. Tejas et. al. [4] investigated the effect of misalignment on vibration response of coupled rotors. They modelled the coupled rotor system using Timoshenko beam elements with all six dof. They found that the misalignment couples vibrations in bending, longitudinal and torsional modes. They also presented experimental investigations for validating the results [5]. Dimarogonas and Papadopoulos [6] investigated the vibration of cracked shafts in bending. They obtained analytical solutions for the closing crack under the assumption of large static deflections, a situation common in turbomachinery. Vibration and stability of a rotating shaft containing a transverse crack was studied by Huang et. al. [7]. The steady state responses and the stability criteria were obtained, and the effects of crack depth, crack location and rotational speed were discussed. It is found that the crack affects the dynamic response more significantly when it occurs near a place where the bending moment exhibits a larger value. Also the investigations of the dynamics of a rotor system with bearing clearance are presented by Flowers et. al. [8]. Akturk [9] presented some characteristic parameters affecting the natural frequency of a rotating shaft supported by defect-free ball bearings. He presented a new analytical investigation into the effects of preload, the number of rolling elements and ball set position. Therefore, it can be observed from these studies that controlling the geometry of shafts and their involved rotating parts is very important and geometric tolerances are more important and effective than dimensional tolerances. This paper investigates the effects of geometric tolerances of rotating shafts on their vibrations. Tolerances of the bearings and the type of adaptation between shaft and bearings are not discussed here, but rigid bearings with no damping effects and friction are considered. Geometric tolerances associated with shafts include straightness, circularity, cylindricity, concentricity, coaxiality, circular run-out (radial) and total radial run-out tolerances [10-12].

Although the results of such an analysis would be useful in any system that has rotating shafts, the present study will be more valuable for very sensitive and high speed systems in which any deviation in critical rotational speed is very important. So far, industrially-developed motors have normally reached 250,000 revolutions per minute [13]. Some rotating shafts are supercritical, which means their rotational speed goes further than the first critical rotational speed. This calls for investigating the effects of the tolerances on natural frequencies higher than the fundamental frequency. This paper aims to show the effects of geometric tolerances, by increasing the natural frequencies and mode shapes.

2. Implementation Method

In this paper three different rotating shafts in terms of size and shape are considered:

- I) A rotating shaft with 50 mm diameter and 500 mm length.
- II) A rotating shaft with 50 mm diameter and 1,000 mm length.
- III) A step shaft including a narrow section with 50 mm diameter and 300 mm length and a stockish section with 66 mm diameter and 600 mm length that is modeled from a real rotating shaft.

In the manufacturing processes of these presented shafts, three types of output deviated surfaces are considered. Specific geometric tolerances should be used for geometry controlling for each of these types. Here the kind of tolerance is less important, because each tolerance may contain another as well, and also different tolerances can be applied to the same type and relatively the same results may be obtained. These types and the related geometric tolerances are depicted in Fig. 1.

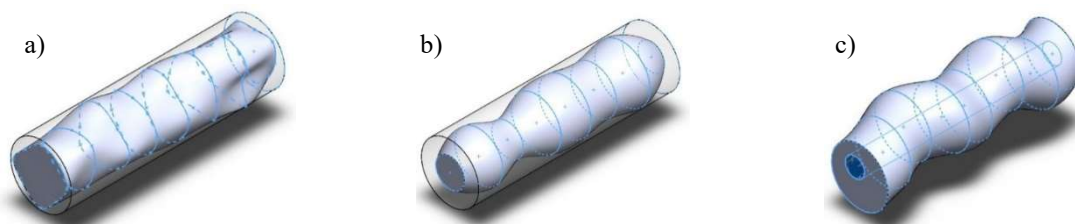


Fig. 1. Exaggerated output surface of manufacturing processes. **a** first manufacturing process – cylindricity tolerance used. **b** second manufacturing process – total radial run-out tolerance used. **c** third manufacturing process – coaxiality tolerance used.

For the first type, the deviations generated from ideal state are applied to specific sections along the axis of rotation by a negative effect so that on each of these sections, based on a specified angle, deviations could be considered on different points of the circumference of the cross section. Therefore, the circumferences of these sections are not uniform circles and have some deviations. For the second type, negative deviations on specific sections along the axis of rotation are applied only to the radius of the section circles. As a result, these sections are uniform circles and they only differ from each other in size. In addition, centers of all these circles are located on the axis of the ideal cylinder (datum axis). For the third type, the deviations are in a way that all sections are uniform circles with a diameter equal to the ideal diameter. However, the deviations are applied to the centers of the sections and the centers are not located on a straight line and have distances from datum axis.

These three mentioned types for machining processes, are applied to the models. Modeling the deviations is done

by generating a set of deviated points with the help of random numbers in MATLAB. Different types of deviations with different tolerance values and different numbers of deviated points are applied to the mentioned rotating shafts. Therefore, the effects of these parameters on the natural frequencies will be investigated too. Furthermore, to enhance the accuracy of the results, several models will be created with the same conditions and the average of the results is considered as the final result. This will reduce the errors. Desired parameters are shown in Fig. 2:

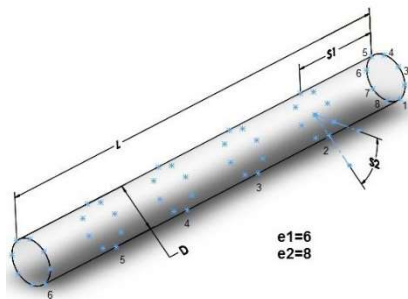


Fig. 2. Displaying considerable parameters on the shaft

where, $e1$ is the number of longitudinal sections and $e2$ is the number of points applying the deviations in every section. For applying the deviations, a parameter called the diametric tolerance coefficient (T_c) will be used that is equal to the ratio of geometric tolerance to the shaft diameter. Thus, for the step shaft with a constant diametric tolerance coefficient, surface deviation ranges of the shaft parts are different.

$$T = T_c \times D \tag{1}$$

For generating random numbers, standard normal distribution (Gaussian distribution) is used in which the probability density function includes $\sigma=0$ and $\mu=1$. The intervals of the numbers generated by this function are infinite, so for limiting them only those in the range of $[\sigma-3\mu, \sigma+3\mu]$ are acceptable. This range includes more than 99.7% of the total generated numbers, so its error can be neglected.

For example, if the input for the diametric tolerance coefficient is 0.01 and the diameter of the shaft is 50mm, then the tolerance equals to 0.5mm, which means the maximum deviation between the ideal and generated points is 0.5mm. After generating the deviated points, they are imported into the SolidWorks software. It is necessary to create closed curves passing through the points on the same longitudinal plane. After passing a cylindrical surface through these section curves, the external surface of the shafts may be created and finally the solid model could be created easily.

3. Analyzing the Models

Finite element method is used for estimating the natural frequencies. For this purpose, Ansys the commercial FE software is used. Two dimensional quadratic order surface elements are used. Shafts are made of steel with the following characteristics:

Table 1. Physical characteristics of presented shafts

Module of elasticity (N/m^2)	Poisson's ratio	Density (Kg/m^3)
$E = 2.1 \times 10^{11}$	$\nu = 0.3$	$\rho = 7800$

For finding the appropriate number of nodes for meshing, it is necessary to perform mesh sensitivity test for every shaft. The results of this test for rotating shaft (I), is shown in Fig. 3. It is observed that the slope of the curve is decreasing, so the selection of approximately 10,000 nodes for the shaft (I) is suitable.

Referring to Fig. 4, three main loads are applied to the rotating shafts: first gravity, second the reaction forces exerted by constraints such as bearings, and third the transverse forces applied to the shaft playing the role of components installed on the shaft such as gears. Shafts are often constrained on both sides. They are directly connected or coupled to the drive shaft or electric motor from one side. Although the support is clamped in reality but for illustrating the effects of tolerances, boundary conditions are merely considered as simply supported. Boundary conditions for the rotating shafts (I) and (II) are simply supported with the possibility of longitudinal motion. Thus, one side is constrained in three directions and the other side only in two transverse directions. The same boundary conditions are applied to the shaft (III) and because it is a step shaft, the second bearing is located at the step. The boundary conditions are applied to the model using Ansys as shown in Fig. 4.

Performing the static analysis and subsequently the modal analysis [14], we would obtain the results including natural frequencies, mode shapes and also the relative displacements. From eq. (2) it can be observed that the torsional natural frequency ω_n of the shaft is independent of the diameter and just is a function of shear modulus G , density ρ and length L of the shaft [15].

$$\omega_n = \sqrt{\frac{k_\theta}{J}}, J = \frac{1}{2} mR^2, m = \pi\rho R^2 L \tag{2}$$

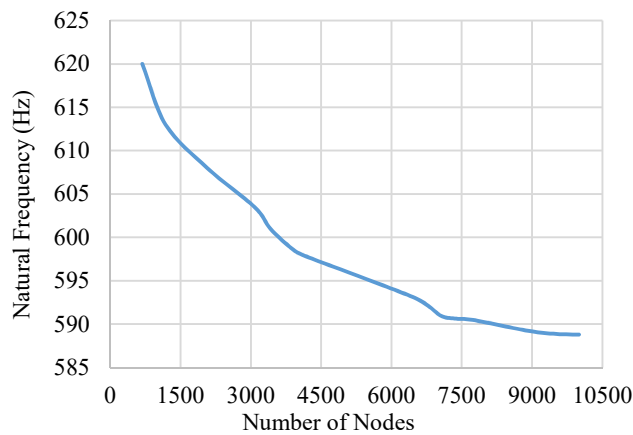


Fig. 3. Mesh sensitivity graph of the first bending mode shape of ideal shaft (I)

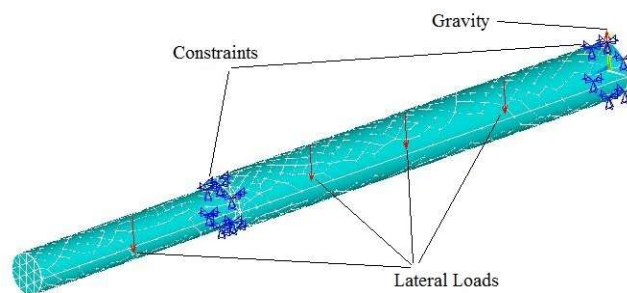


Fig. 4. Applying forces on rotating shaft (III)

It can also be observed from the results that the effects of geometric tolerances on the natural frequencies of torsional and longitudinal mode shapes, are negligible. Thus, only natural frequencies of the bending mode shapes will be studied.

4. Results & Discussions

Mode shapes of rotating shafts (II) and (III) are presented in appendix. Due to the geometrical similarity of shafts (I) and (II), their mode shapes are also similar; thus, the mode shapes of shaft (I) are not presented. The values of natural frequencies of ideal rotating shafts are listed in Table 2:

Table 2. Natural frequencies of ideal shafts

Bending mode shape number	Natural frequencies (Hz)		
	Shaft (I)	Shaft (II)	Shaft (III)
1	588.78	153.33	388.58
2	1849.1	493.17	760.54
3	3668.5	1015.3	1991.5
4	5890.5	1704.4	2254.8
5	-----	2541.8	-----

It can be seen that natural frequency difference between the ideal and deviated shafts follow a particular rule for bending mode shapes. Applying deviations negatively on the rotating shafts will always result in decreasing the natural frequencies. As can be seen from Figs. 5 & 6, difference values constitute a particular percentage of natural frequencies of ideal models and the percentages are nearly identical for different types of deviations and natural frequencies. It is observed that the results for the cylindricity and total run-out tolerances for the same tolerance value are slightly different. As the geometric tolerance value goes higher, difference percentage goes higher too. The results are computed from the average results related to different cases with different numbers of deviation applying points but the same tolerance coefficients.

The ratio between difference percentages and diametric tolerance coefficients are computed and the related results for all shafts are presented in Figs. 7, 8 and 9. The ratio is a dimensionless number and does not have a physical meaning, but it can be seen that for each shaft with different diametric tolerance coefficients, the results are approximately the same. Also it should be noted that the ratio is approximately equal for different kinds of shafts which is here nearly equal to 60. Designers can use the results to estimate the difference values of natural frequencies of real

and ideal shafts for different support conditions and tolerances.

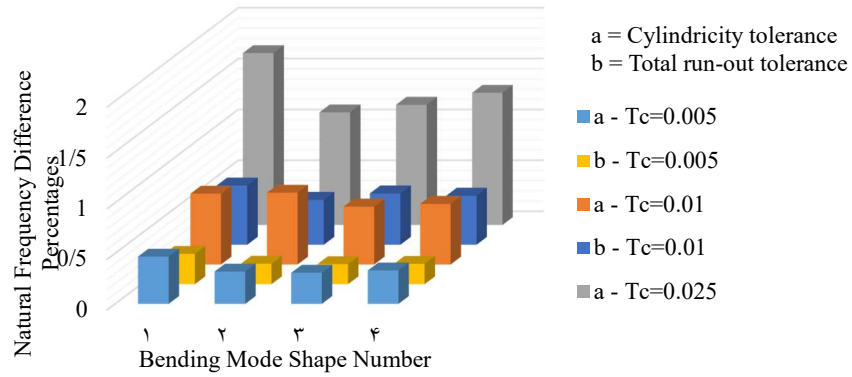


Fig. 5. Comparing natural frequency difference percentages for different cases of shaft (I)

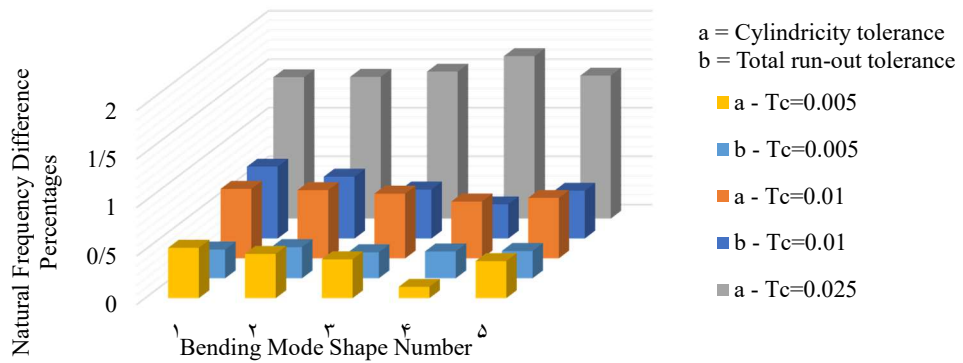


Fig. 6. Comparing natural frequency difference percentages for different cases of shaft (II)

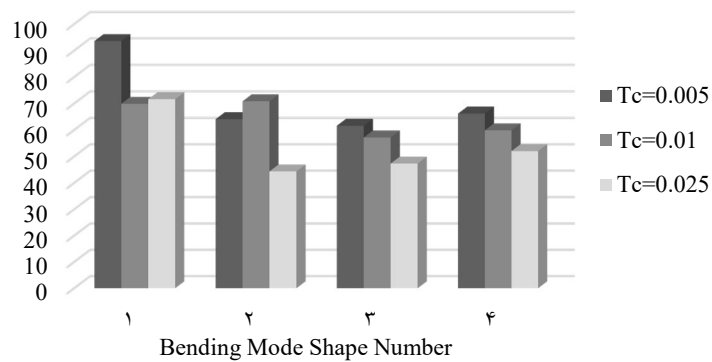


Fig. 7. Comparing the ratio between natural frequency difference percentages and diametric tolerance coefficients for different cases of shaft (I)

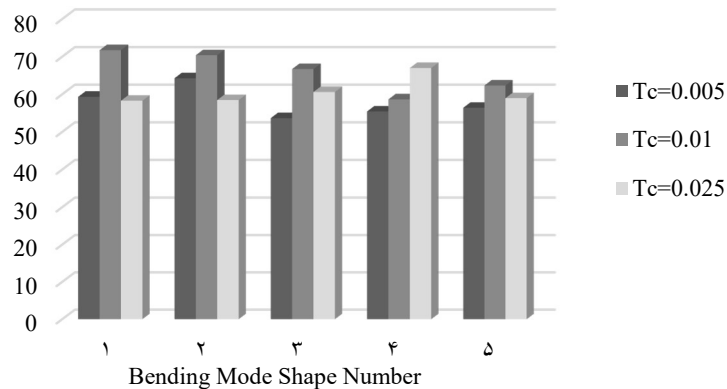


Fig. 8. Comparing the ratio between natural frequency difference percentages and diametric tolerance coefficients for different cases of shaft (II)

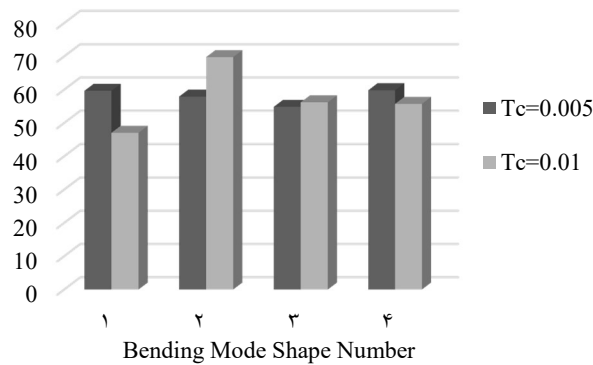


Fig. 9. Comparing the ratio between natural frequency difference percentages and diametric tolerance coefficients for different cases of shaft (III)

As mentioned before, to enhance the accuracy, the average of the results were presented. In this case, the mean value alone is not sufficient and the data distribution around the mean value should be presented. For example, the output results related to the first natural frequency of shaft (I) with $T_c=0.005$ are presented in Fig. 10. Running the written code for several times would result in different sets of points. As shown, the horizontal axis shows the difference percentage of natural frequencies between the output values and the mean value. The vertical axis only shows the compactness of the points regarding the mean value. As depicted, where the points are compact, the curve goes upward and where the points are expanded, the curve goes downward. The trend of the points is approximated by the normal density function. Therefore, as the input applied deviation was based on the normal distribution, the output results are distributed regarding the mean value based on the normal distribution too.

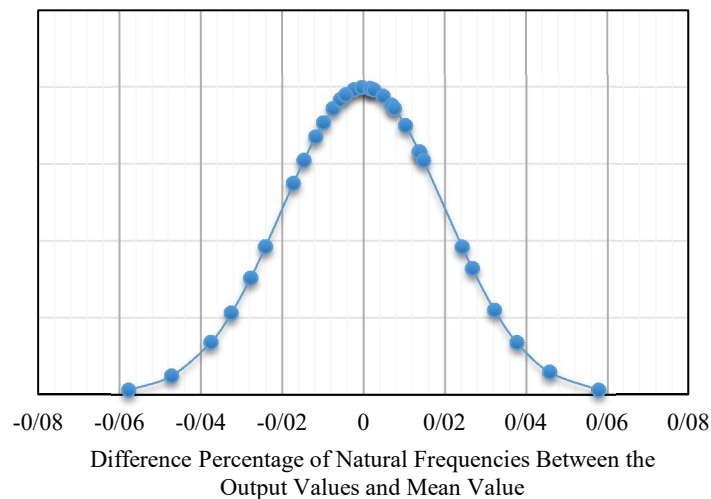


Fig. 10. Distribution curve of output results of the first natural frequency of shaft (I) with $T_c=0.005$ about the mean value.

By comparing Fig. 10 with Fig. 11 that is a normal density function, it can be concluded that the standard deviation of the normal curve in Fig. 10 is about 0.02. Therefore, about 68% of the results have up to 0.02% difference from the mean value and about 27% of the results are 0.02% to 0.04% different, and the rest of the points are about 0.04% to 0.06% different from the mean value.

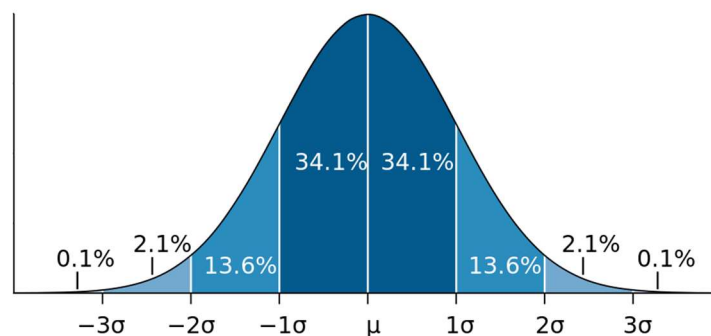


Fig. 11. Normal density function with related probability ranges [16]

Table 3 shows the simple variances of output results for the first three bending mode shapes of shaft (I) with $T_c=0.005$. The first row is related to the points presented in Fig. 10. As can be seen, the values of simple variances of natural frequencies are little that means the results are compact about the related mean values. As shown the values of simple variances of difference percentages of natural frequencies are close to each other, which means the distribution of the results related to the second and the third mode shapes are like the those of the first mode shape and therefore Fig. 10 is nearly identical for all bending mode shapes of the rotating shaft.

Table 3. Simple variances of output results of first three bending mode shapes of shaft (I) with $T_c=0.005$

Bending mode shape number	Simple variance of natural frequencies	Simple variance of difference percentages
1	0.023434	0.000676
2	0.222588	0.000651
3	0.846501	0.000629

The results of the deviation applying related to the third type of manufacturing process show that frequency difference values of the bending mode shapes are always negative as in the previous types, but these difference values are very small and can be neglected. This is obvious when considering the shape of the shaft and slight distance between the bearings. That is why the results are not presented for this type of applying deviations. Mean result values for all shafts for different diametric tolerance coefficients are shown in Fig. 12. It can be seen that the critical rotational speed difference between the ideal and real shafts, nearly does not depend on the kind of shafts and is only related to the natural frequency of ideal models. In general, it can be stated whenever the natural frequency is higher, the difference is higher too. These differences can be roughly approximated by straight lines. It can be observed that increasing the diametric tolerance coefficient would also increase the slope of approximation lines, which means the increase of the critical rotational speed differences between the ideal and real values.

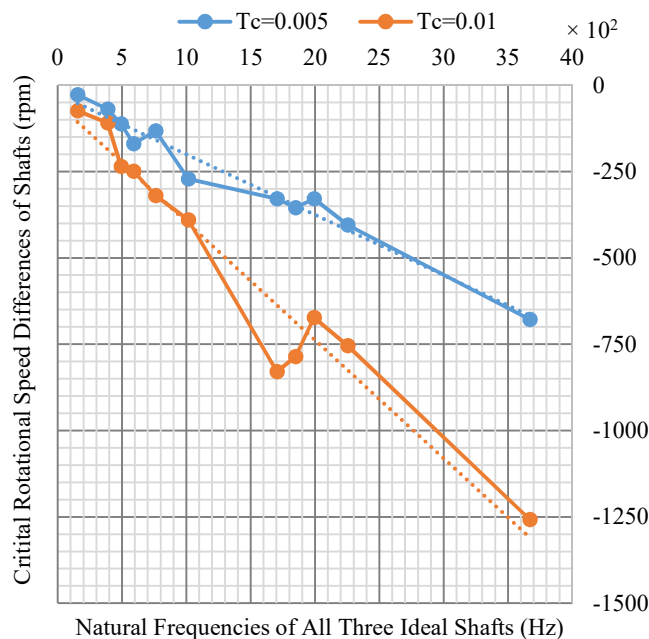


Fig. 12. Critical rotational speed differences between ideal and real shafts vs. natural frequencies of related ideal shafts

5. Conclusion

In this paper an attempt was been made to investigate the relation between the natural frequencies of rotating shafts and the related geometric tolerances. Three rotating shafts with different sizes and geometries were considered. By applying different geometric tolerances in the form of shaft surface deviations by a completely random method, their effects on the natural frequencies were determined using the finite element simulation software. The results show that whenever the natural frequency of the shafts increases, natural frequency difference between ideal and deviated surface models increases almost linearly too. Also as expected, increasing the geometric tolerances would result in increasing the difference values. It follows that this difference value is equal to a specific percentage of natural frequency of the related mode shape. For a given rotating shaft, the percentage value is almost constant for all mode shapes. The ratio between the difference percentage and diametric tolerance coefficient is almost independent of the value of tolerance coefficient and the kind of rotating shaft.

Acknowledgments

The authors would like to express their thanks and appreciations to the Khavar Rotating Machinery Engineering Co. for their cooperation in this study.

Nomenclature

D	Diameter of the shaft [m]	T	Geometric tolerance [m]
E	Module of elasticity [N/m ²]	T_c	Diametric tolerance coefficient
G	Shear modulus [N/m ²]	Greek Symbols	
I	Area moment of inertia (polar) [m ⁴]	θ	Torsional angle [rad]
J	Mass moment of inertia [Kg.m ²]	μ	Standard deviation
K_θ	Torsional rigidity [N/rad]	ν	Poisson's ratio
L	Length of the shaft [m]	ρ	Density [Kg/m ³]
m	Mass [Kg]	σ	Mean (mathematical expectation)
M	Force moment [N.m]	ω_n	Natural frequency [rad/s]
R	Radius of the shaft [m]		

Appendix

Vibrating mode shapes related to shafts (II) and (III) are shown in below:

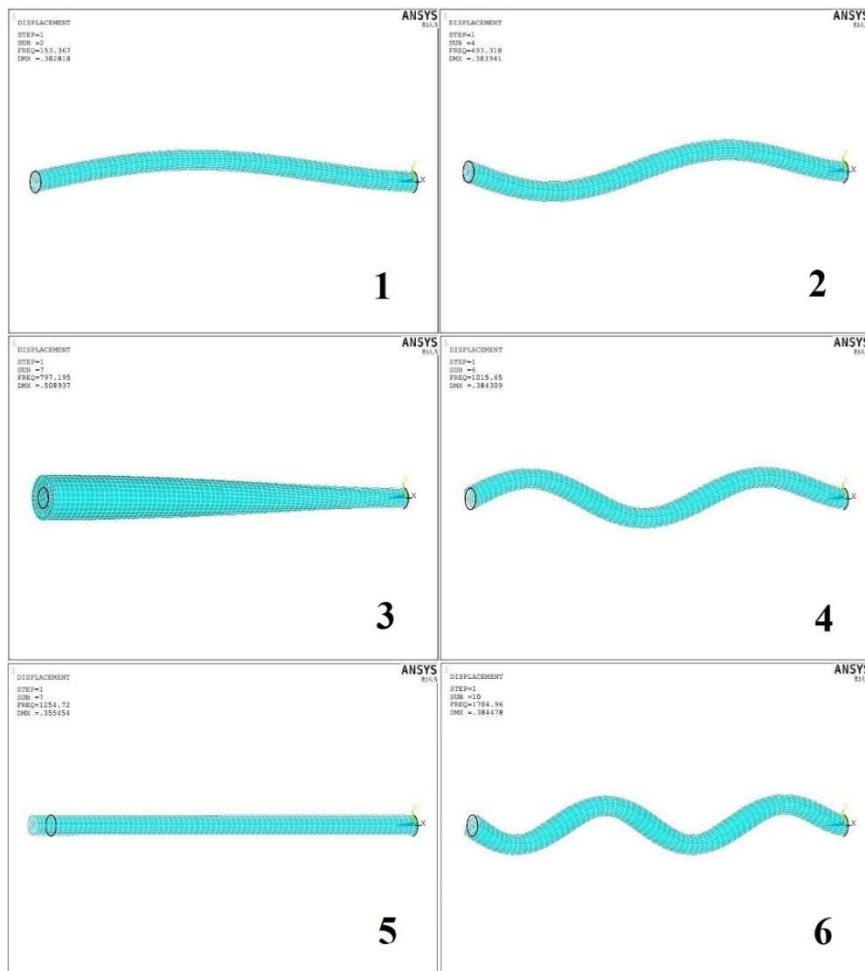


Fig. 13. Mode shapes of shaft (II). Mode shapes 1, 2, 4 & 6 are first four bending vibrating modes. Mode shapes 3 & 5 are the torsional and longitudinal vibrating mode shapes respectively.

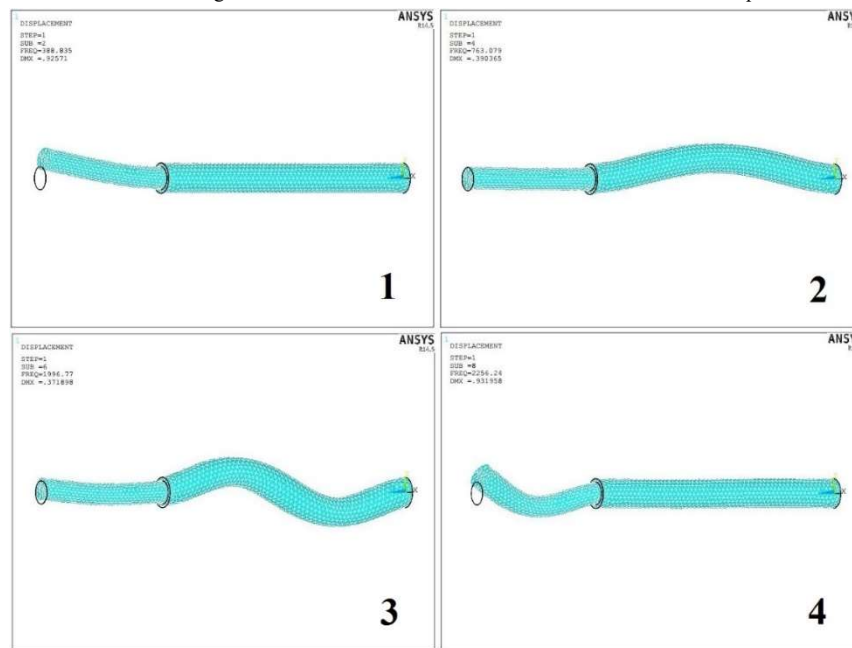


Fig. 14. First four bending mode shapes of shaft (III)

References

- [1] Xu, M., Marangoni, R. D., "Vibration Analysis Of A Motor-Flexible Coupling-Rotor System Subject To Misalignment And Unbalance, Part I: Theoretical Model And Analysis", Journal of Sound and Vibration, Vol. 176, No. 5, pp. 663-679, 1994.
- [2] Xu, M., Marangoni, R. D., "Vibration Analysis Of A Motor-flexible Coupling-Rotor System Subject To Misalignment And Unbalance, Part II: Experimental Validation", Journal of Sound and Vibration, Vol. 176, No. 5, pp. 681-691, 1994.
- [3] Lee, Y. S., Lee, C. W., "Modelling and Vibration Analysis of Misaligned Rotor-Ball Bearing Systems", Journal of Sound and Vibration, Vol. 224, No. 1, pp. 17-32, 1999.
- [4] Patel, T. H., Darpe, A. K., "Vibration response of misaligned rotors", Journal of Sound and Vibration, Vol. 325, No. 3, pp.609-628, 2009.
- [5] Patel, T. H., Darpe, A. K., "Experimental investigations on vibration response of misaligned rotors", Mechanical Systems and Signal Processing, Vol. 23, No. 7, pp. 2236-2252, 2009.
- [6] Dimarogonas, A. D., Papadopoulos, C. A., "Vibration of Cracked Shafts in Bending", Journal of Sound and Vibration, Vol. 91, No. 4, pp. 583-593, 1983.
- [7] Huang, S. C., Huang, Y. M., Shieh, S. M., "Vibration And Stability Of A Rotating Shaft Containing A Transverse Crack" Journal of Sound and Vibration, Vol. 162, No. 3, pp. 387-401, 1993.
- [8] Flowers, G. T., Fansheng Wu, "Disk/Shaft Vibration Induced by Bearing Clearance Effects: Analysis and Experiment", ASME Journal of Vibration and Acoustics, Vol. 118, No. 2, pp. 204-208, 1996.
- [9] Akturk, N., "Some Characteristic Parameters Affecting the Natural Frequency of a Rotating Shaft Supported by Defect-Free Ball Bearings", Journal of Multi-Body Dynamics, Vol. 217, No. 2, pp. 145-151, 2003.
- [10] Hertzold, G., Handbook of Geometrical Tolerancing: Design, Manufacturing and Inspection, John Wiley & Sons, New York, 1999.
- [11] ISO 1101, Geometrical Tolerancing, International Organization For Standardization, Switzerland, 1st Edition, 1983, See also URL <http://www.iso.org>
- [12] ASME Y14.5, Dimensioning and Tolerancing, The American Society of Mechanical Engineers, New York, 1994, See also URL <https://www.asme.org>
- [13] Kolar, J. W., "ETH Zurich Researchers and Industry Break World Record", On the WWW, November, 2008, URL <http://www.eurekalert.org>.
- [14] Swanson, E., Powell, C. D., Weissman, S., "A Practical Review of Rotating Machinery Critical Speeds and Modes", Journal of Sound and Vibration, Vol. 12, No. 11, pp. 91-100, 1991.
- [15] Thomson, W. T., Mechanical Vibration, George Allen and Unwin, Australia, 1st Edition, 1950.
- [16] Soong, T. T., Fundamentals of Probability and Statistics for Engineers, John Wiley and Sons, New York, 2004.